Proceedings of the 8th International Conference on Probabilistic Method Applied to Power Systems
Iowa State University, Ames, Iowa, Sept. 12-16, 2004

Coping with Multiple Q-V Solutions of the WLS State Estimator Induced by Shunt-Parameter Errors

Serge Lefebvre, Jacques Prévost, Hans Horisberger, Bertrand Lambert, Lamine Mili

Abstract - The paper proposes a new iterative algorithm able to cope with multiple Q-V solutions of the WLS state estimator due to shunt-reactance errors. For such errors, it is shown in a 735/230-kV Hydro-Quebec subsystem that the conventional Gauss-Newton iterative algorithm converges to a strongly biased Q-V solution that is not detected as such by the residual statistical tests. By contrast, under no bad measurements, the new iterative algorithm converges to a solution foreseen by the dispatcher via the inclusion of additive state voltage weights in the gain matrix.

Keywords- Power Systems, State estimation, shunt parameter errors, topology errors, multiple Q-V solutions.

I. Introduction

Hydro-Québec has a very unique transmission network. With more than 11000km of 735kV lines and main generation plants located more than 1000km away from the consumption centers, this network is prone to large poorly damped transient and dynamic oscillations, yielding acute angular and voltage stability problems. To improve the voltage stability margins of the system, a host of voltage-support equipment such as series compensators, static compensators, shunt capacitors and inductors, and synchronous condensers has been installed on the network over the years. One consequence of this overcompensation is the appearance of a large circulation (absorption and consumption) of reactive power throughout the transmission network. For example, the total shunt generation of reactive power on the 735kV lines is in the same order of magnitude than the total real power injection, typically around 33000MVAr. To be able to set the nodal voltages within acceptable limits, the operators have at their disposal about 25000MVAr of switched inductors, 13000MVAr of switched capacitors, 12000MVAr of series compensators, and a collection of static compensators and synchronous condensers in the range of -3800 and 5800MVAr.

S. Lefebvre and J. Prévost are with Institut de recherche d'Hydro-Québec, Varennes, Québec, J3X1S1. (e-mail : lefebvre.serge@ireq.ca , prévost.jacques@ireq.ca); H. Horisberger and B. Lambert are with the TransÉnergie, division of Hydro-Québec, Montréal, Québec (horisberger.hans@hydro.qc.ca, lambert.bertrand.2@hydro.qc.ca), L. Mili, is with Department of ECE, Virginia Tech, Alexandria Research Institute, Alexandria, VA 22314, (lmili@vt.edu).

This paper discusses the results of a study carried out through simulations of the sensitivity of the Pδ-QV decoupled WLS state estimator to various uncertainties in the model of the reactive compensation devices on the Hydro-Quebec HV Subsystem. It is found that the Q-V portion of the decoupled normal equation suffers from multiple solutions in presence of shunt parameter errors, induced for example by errors in the breaker positions of shunt inductor banks. In many of these cases, it is observed that the Gauss-Newton iterative algorithm converges to a strongly biased Q-V solution that is not detected by the residual statistical tests, even when the measurement redundancy is high and the measurement accuracy is excellent. Note that the P-δ solution does not suffer from this drawback.

Other more common sources of undetected inaccuracies of the Q-V state estimator solutions are errors in the tap positions of multiple transformer load-tap changers [1-3], errors due to the non-inclusion in the network model of corona losses [4,5], topology errors [6], mutual line impedances and three-phase imbalances [7], to cite a few. For the latter, Hansen and Debs showed in [7] how the solution accuracy can be enhanced by making use of a three-phase state estimator based on an improved modelling of Δ/Δ transformers positive sequence. Even gross errors affecting reactive power measurements (e.g. sign errors) may sometimes pass unnoticed by the state estimator. They may remain so for a long time because system operators do not in general scrutinize as closely the reactive powers as they do for the active powers.

Obviously, improving the quality of the Q-V solution is of utmost importance for all advanced applications such as loss reduction, maximum transfer capability optimization as well as for real-time security assessment. Because presently most of the utilities utilize the WLS state estimator, we propose to add a weight matrix to the Q-V component of the Gauss-Newton gain matrix to drive the iterative algorithm to a Q-V solution foreseen by the dispatcher, should that solution exists. This solution algorithm is termed the Dispatcher-WLS method or DWLS for short. Interestingly, the DWLS gives the same answer as the standard WLS method under no parameter or topology errors and improves on the numerical stability of the Gauss-Newton algorithm in presence of such errors.

The paper is organized as follows. Sections II and III deal with the accuracy of the P-δ and Q-V solutions of the WLS estimator. Section IV describes some simulation results carried out on a Hydro-Quebec subsystem and analyzes the impact that a shunt parameter error has on the WLS solution. An estimation error analysis under shunt parameter error is reported in Section V and the proposed DWLS algorithm is proposed and assessed in Section VI.

II. WLS Static State Estimator

The static state estimator is a basic power system operational tool in an energy management system since its role is to provide a complete, coherent, and reliable base-case power flow solution for contingency analysis, spot price calculation, and load forecasting function, among others.

The inputs to the state estimator are a redundant collection of measurements and a mathematical model that relates these measurements to the nodal voltage magnitudes and phase angles, which are taken as the state variables of the system. This model is based on Kirchhoff's and Ohm's laws and relies on several assumptions, which are: (1) random measurement errors that are Gaussian and uncorrelated with zero mean and known diagonal covariance matrix, $R = \text{diag}(\sigma_i^2)$; (2) a balanced three-phase system, (3) no time-skew between the metered values, (4) the exactness of the pi-equivalent models of the lines and transformers of their parameters, and (5) a known topology of the network. The latter is determined by a topology processor from the metered or given status of the circuit breakers of the system equipments such as lines, transformers, capacitors and inductors, FACTS devices, to name a few.

By making use of this network model, the state estimator provides estimates for all the metered and non-metered P, Q, V and δ network variables. Unlike the metered values, the estimates exactly satisfy Kirchhoff's current and voltage laws and AC Ohm's laws. Furthermore, under the exact fulfillment of the assumptions, including the assumptions made on the measurements' errors, these estimates are also more accurate than their respective metered values since their variances are smaller.

A general state estimation model is given by

$$z = h(x) + e , \tag{1}$$

where z is the measurement vector, e is the measurement error vector, and $h(*)$ is a vector-real valued function. The latter is derived from the foregoing assumptions; in particular, it depends on the given values for the line and transformer parameters and the given network topology. Because the state estimator does not question the exactitude of the function $h(x)$, it transfers any error in $h(x)$ to the measurement error, e. In other words, any error in $h(x)$ will be seen by the state estimator as an error in z, making the vector e to account for errors in both z and $h(x)$. A better model on which to derive a state estimator would be the one that includes an error, e_h, in the argument of the function h(*), yielding

$$z = h(x, e_h) + e . \tag{2}$$

Many commercial software packages seeks a solution to the WLS normal equation,

$$H^T R^{-1} (z - h(x)) = 0, \tag{3}$$

through the Gauss-Newton iterative algorithm given by

$$\Delta x^{(k)} = (H^T R^{-1} H)^{-1} H^T R^{-1} \Delta z^{(k)} , \tag{4}$$

where $H = \partial h(x)/\partial x$ is the Jacobian matrix, $\Delta z^{(k)} = z - h(x^{(k)})$ is the residual vector, and $\Delta x^{(k)} = x^{(k+1)} - x^{(k)}$ is the increment of the state vector at the kth iteration step. The error covariance matrix of the state estimates and of the estimates associated with the measurements are respectively given by

$$\text{Cov}(\delta_x) = \Sigma_x = (H^T R^{-1} H)^{-1}, \tag{5}$$

$$\text{Cov}(\delta_z) = \Sigma_z = H (H^T R^{-1} H)^{-1} H^T . \tag{6}$$

The diagonal elements of Σ_x and Σ_z are the variances of the estimate errors. Under the assumptions stated earlier and under the validity of the linear approximation of the model given by (2) around the solution, these variances provide a measure of the accuracy of the estimates; the smaller they are, the more accurate the state estimator solution is.

III. Analysis of the P-δ and Q-V Solutions

This section reports on the typical performance of the fully decoupled WLS state estimator on the 735-kV Hydro-Quebec subsystem. This performance will be measured by means of three different indices, α, β, and γ, which are defined as follows. Let m be the total number of measurements, let m_e denote the number of measurements deleted by the bad data identification procedure, N be the number of buses, and n = N - 1 denote the number of the state variables. Let $\hat{z}_i$ denotes the estimate associated with the ith measurement and $r_{Wi} = (z_i - \hat{z}_i)/\sigma_i$ be the corresponding weighted residual. Then, define

$$J(\hat{x}) = \sum_{i=1}^{m-m_e} r_{Wi}^2 , \tag{7}$$

$$J_{mean} = (m - m_e) - n , \tag{8}$$

$$\alpha = J(\hat{x}) / J_{mean} , \tag{9}$$

$$\beta = \left| \sum_{i=1}^{m-m_e} r_{Wi} \right| , \tag{10}$$

$$\gamma = m_e / m . \tag{11}$$

The index α given by (9) is the ratio of the estimated value of the WLS objective function upon completion of the bad data elimination procedure to the theoretical mean value of that objective function under the strict fulfillment of the assumptions. If the assumed values for $\{\sigma_1 , \ldots, \sigma_m\}$ are good approximations of the standard deviations of the actual measurement errors, then the mean value of the index α is around 1. On the other hand, a much larger value of that mean would be indicative of a strong mismatch between the measurement and the model.

Concerning the index β given by (10), it is proportional to the solution bias since under the strict fulfillment of the assumptions, $E[r_w] = 0$. We infer that the mean value of β is around zero when the solution is unbiased. As for the index γ given by (11), it is the fraction of rejected measurements. Since all the P and Q measurements come in pairs and are obtained via the same data acquisition chain (PT, CT, transducers, A/D converters), the numbers of rejected P and Q measurements are expected to be of the same order.

Typical values for these indices are displayed in Table I for a 90-bus 735-kV Hydro-Quebec subsystem. This table clearly shows that all the indices of the Q-V solution are 7 to 8 times higher than those of the P-δ solution. Clearly, the accuracy of the P-δ solution is superior to that of the Q-V solution.

TABLE I
Typical index values for a 90-bus Hydro-Quebec HV system.

	m	α	β	γ
P-δ	231	0.29	3.4	0.01
Q-V	267	2.08	27.7	0.08
Q	231	2.46	22.2	0.08
V	36	0.81	5.5	0.00

IV. SIMULATION RESULTS: IMPACT OF A SHUNT PARAMETER ERROR ON THE WLS SOLUTION.

To study the impact of shunt parameter errors on the WLS solutions, some simulations have been carried out on a small 735/230-kV 8-bus subsystem of Hydro-Quebec whose one-line diagram is depicted in Fig. 1. As seen in this figure, the sub-network consists of a single 735-kV transmission line connected to a 230-kV subsystem possessing five transmission lines. The system is provided with a high measurement redundancy of 3.47 since all the 8 buses are each equipped with a voltage measurement and a pair of P and Q power injection measurements and all the 7 branches (6 lines and one transformer) have each a pair of P and Q power flow measurements on both sides, yielding a total of 52 measurements for 15 state variables. The system is of small size but reproduces the phenomena observed in the complete model of the Hydro-Quebec system, which includes more corridors and loops.

A parameter error has been introduced in the model of the 50-MVar shunt-reactor connected to Bus m230. Specifically, the reactor is assumed to be off while it is in fact on. Table II displays the estimated Q-V variables obtained. Interestingly, the changes in the gain matrix are small when the shunt reactor is connected and disconnected. This table reveals that the voltage measurement, V_{m735}, at Bus m735 has the largest absolute weighted residual of 3.087, just above the threshold of 3, although its measured value is only at one standard deviation away from its true value. This means that the error on V_{m735} is amplified. In fact, the estimator provides strongly biased voltage estimates.

If V_{m735} is deleted, then all the absolute values of the weighted residuals become smaller than 1 and the χ^2-statistical test on the criterion J(x) becomes insignificant. In other words, the residual tests fail to reveal the presence of the shunt parameter gross error although the voltages V_{k735} and V_{m735} are estimated at values of 1.001 pu and 1.047 p.u., which are

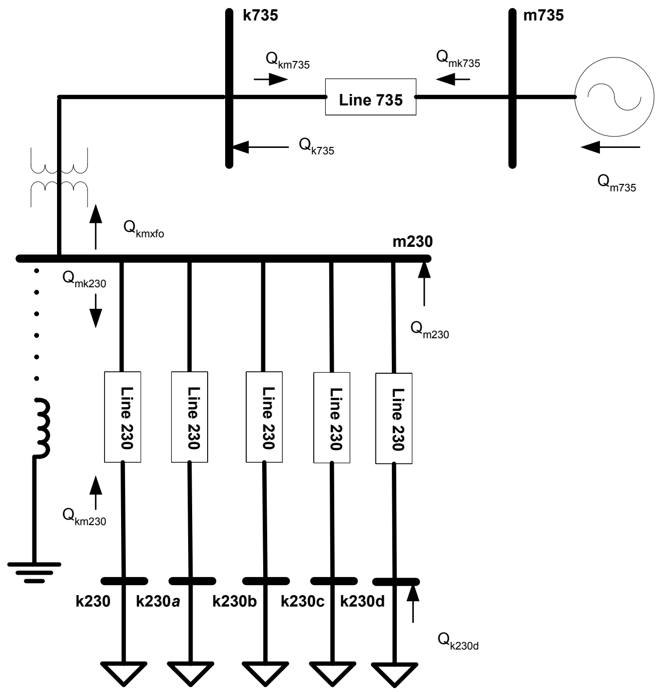

	R_{series} (p.u.)	X_{series} (p.u.)	B_{shunt} (p.u.)
735-kV lines	0.00055	0.01558	7.19586
230-kV lines	0.001150	0.01942	0.04049
Transformers	0.0000765	0.00880	0.00000

Fig. 1. Hydro-Quebec 735/230-kV subsystem.

unacceptable for the dispatcher since they are much less accurate than the metered values of 0.992 p.u. and 1.010 p.u., respectively. Note that the true values are 0.992 p.u. and 1.021 p.u., respectively.

One might think that by adding one reactive power flow measurement, Q_{mk735}, with $\sigma = 0.4$ pu, the quality of the estimates would improve and the detection test would reveal the presence of the shunt parameter gross error. This hope does not come true since this increase in the reactive measurement redundancy does not affect the voltage estimates on the 735kV network; the latter remain nearly unchanged at strongly biased values. In fact, one way to correct them is to significantly decrease the standard deviation σ_{Q735} on the reactive injection measurement, Q_{k735}. But this option is not accepted by the dispatcher on the ground that this decrease yields an unrealistic low value for σ_{Q735}. This dilemma calls for another solution to this problem, which will be proposed in Section VI. Note that unlike the Q-V solution, the P-δ solution is good.

V. ESTIMATION ERROR ANALYSIS UNDER A SHUNT PARAMETER ERROR

To investigate the degradation of the bias of the estimates under shunt parameter errors, a performance index is to be defined. In this study, we define this index for the *ith* estimate

TABLE II
WLS solution with shunt parameter error at bus m230.

z	true	measured	estimed	r_w
Q_{km735}	-3.666	-4.466	-4.794	0.820
Q_{mk735}	-1.131		-0.042	
Q_{k735}	0.000	0.000	0.000	-0.001
Q_{m735}	1.131		0.042	
V_{k735}	0.992	0.992	0.996	-0.341
V_{m735}	***1.021***	***1.010***	***1.042***	***-3.087***
Q_{km230}	-0.000	-0.080	-0.059	-0.514
Q_{mk230}	0.148	0.228	0.206	0.549
Q_{k230}	0.000	0.040	0.059	-0.486
Q_{m230}	0.000	0.000	0.000	-0.004
V_{k230}	0.969	0.974	0.962	1.252
V_{m230}	0.974	0.974	0.968	0.635
Q_{km230a}	-0.000	-0.060	-0.047	-0.319
Q_{mk230a}	0.148	0.228	0.194	0.857
Q_{k230a}	0.000	0.020	0.047	-0.681
V_{k230a}	0.969	0.964	0.962	0.227
Q_{km230b}	-0.000	-0.060	-0.033	-0.677
Q_{mk230b}	0.148	0.168	0.179	-0.281
Q_{k230b}	0.000	0.040	0.033	0.177
V_{k230b}	0.969	0.974	0.962	1.198
Q_{km230c}	-0.000	0.020	0.009	0.285
Q_{mk230c}	0.148	0.128	0.137	-0.235
Q_{k230c}	0.000	0.030	-0.009	0.965
V_{k230c}	0.969	0.959	0.963	-0.386
Q_{km230d}	-0.000	-0.040	-0.020	-0.495
Q_{mk230d}	0.148	0.188	0.166	0.540
Q_{k230d}	0.000	0.000	0.020	-0.505
V_{k230d}	0.969	0.969	0.962	0.672
Q_{kmxfo}	-1.214	-2.014	-2.287	0.683
Q_{mkxfo}	2.681		3.802	

as 1.4827 times the median of the absolute value of the estimate error divided by the assumed standard deviation of the corresponding measurement error, that is,

$$1.4826 \text{ Median } \{|z_{i,true} - \hat{z}_i| / \sigma_i\}. \quad (12)$$

Here the median is taken over a large number of state estimation runs with randomly generated measurement errors following a Gaussian distribution with zero mean and an assumed variance, σ_i^2. This ratio is referred to as the measurement error attenuation. Note that the correction factor of 1.4826 included in (12) is needed to make the median of the absolute value of the estimate error equal to its standard deviation under no parameter errors. An alternative definition of this index would be the mean-square value of the weighted estimate error. Obviously, an attenuation smaller than 1 indicates that the corresponding estimate is more accurate than the associated metered value while an attenuation larger than 1 indicates the presence of a bias in the estimate. The attenuation of a critical measurements is equal to 1 in all cases because we have $\hat{z}_i = z_i$.

Fig 2 displays the locus of the weighted residual of the bus voltage measurement V_{m735} as the standard deviations, σ_{Q230}, of

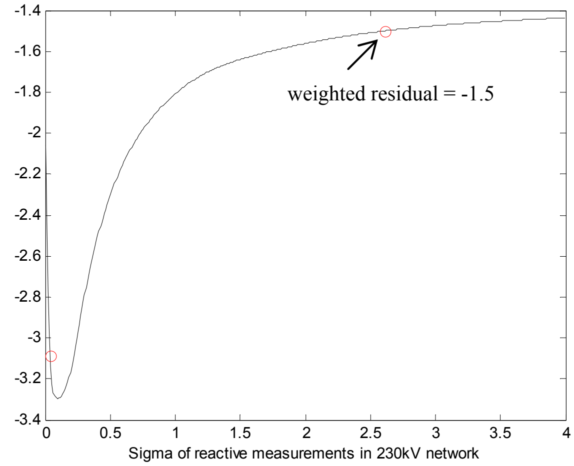

Fig. 2. Variation of r_w versus σ_{Q230} for $\mathbf{V_{m735}}$.

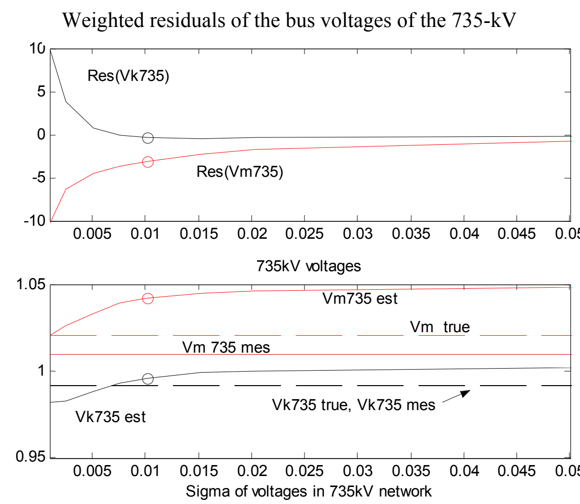

Fig. 3. Weighted residuals and bus voltage estimates versus σ_{V735} for the 735-kV system

the 230-kV reactive power measurements are increased. It is observed that to decrease the magnitude of this voltage weighted residual to 1.5, the standard deviation σ_{Q230} has to grow to 2.6, which is an increase of 65 times its original value of 0.04. Based on meter accuracy, this value for σ_{Q230} is unacceptable for the dispatcher.

Fig. 3 depicts the loci of the weighted residuals r_{Wi} and the bus voltage estimates for the 735-kV system as the standard deviations, σ_{V735}, of the 735-kV voltage measurements are changed from their nominal value of 0.01. At this nominal value, r_{Wi} and the voltage estimates are indicated by circles. As observed, the magnitudes of the voltage weighted residuals increase as σ_{V735} is decreased from its nominal value. On the other hand, as σ_{V735} is increased beyond 0.01, the voltage estimates on bus m735 and k735 move far away from their true values.

Fig. 4 displays the loci of the Q-V total objective function, J_{total}, and its 735-kV and 230-kV components denoted by J_{230}

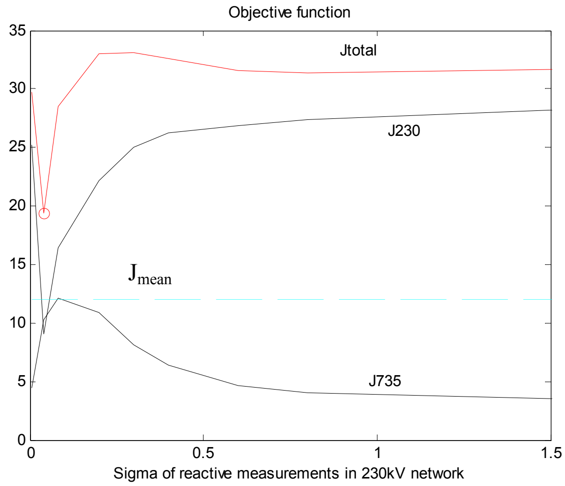

Fig. 4. The Q-V objective function J_{total} and its 735-kV and 230-kV components versus σ_{Q230}.

and J_{735}, respectively, as the standard deviation σ_{Q230} of the 230-kV reactive power measurements is changed. We observe that J_{230} reaches its minimum when the σ_{Q230} is at its actual value of 0.04 p.u while J_{735} attains its maximum for a larger value of σ_{Q230}. But the latter is of no consequence for the minimum value of the Q-V total objective function, J_{total}, since it is attained for the actual value of $\sigma_{Q230.}$ Note that the mean value, J_{mean} , shown in the figure is calculated under the twin assumptions of no modelling errors and no bad measurements.

Fig. 5 displays the loci of the voltage, power flow, and power injection components of the Q-V total objective function J_{total} as the standard deviation σ_{Q230} of the 230-kV reactive power measurements is changed. We observe that around the actual value of σ_{Q230}, the voltage component with 8 terms (8 voltage measurements) contributes more to the objective function than the reactive power flow component with 12 terms (12 Q measurements) and the reactive power injections with 10 terms (8 Q measurements and 2 zero Q injections). While the injections contribution is nearly constant, since the voltages are priorized in the solution, the flows are allowed to deviate.

Table III shows the impact of the shunt parameter error on the error attenuations. The first column displays the theoretical values of the attenuations while the other two columns display the attenuation values obtained via simulations resulting from 5000 state estimation runs. Specifically, column 2 and 3 provide the error attenuations for the case where the shunt parameter error is not present and is present, respectively. As for the measurement errors, they are drawn from independent Gaussian distributions with zero mean and exact variances. Note that the attenuations given in the first and second columns of this table are very close. As expected, the estimates are more accurate than the raw measurements under exact fulfillment of the assumptions. However, as seen in the third column of Table III, the attenuations are much larger than unity for the Q and V estimates of the 735-kV subsystem. It is then clear that estimates for this subsystem are strongly biased.

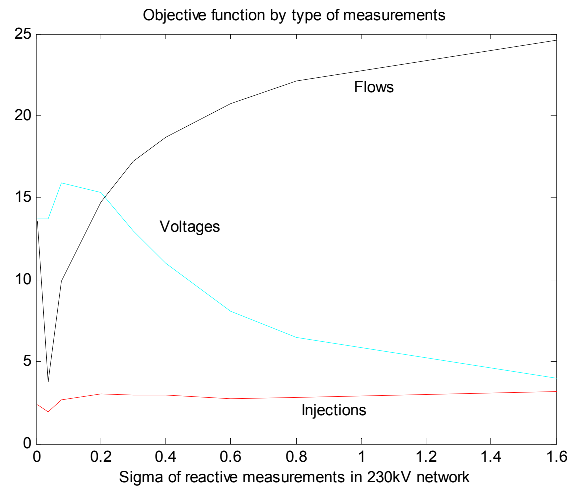

Fig. 5. The voltage, power flow, and power injection components of the WLS objective function J(x) versus σ_{Q230}.

Table III

Error attenuations obtained via 5000 state estimation runs.

z	Theoretical attenuation	Without topology error	With topology error
Q_{km735}	0.1472	0.1433	3.4440
V_{k735}	0.3501	0.3512	0.5389
$\boldsymbol{V_{m735}}$	***0.3755***	***0.3809***	***2.6310***
Q_{km230}	0.5745	0.5663	0.6129
Q_{mk230}	0.5745	0.5827	0.6471
Q_{k230}	0.5745	0.5749	0.6186
V_{k230}	0.3538	0.3598	0.6526
V_{m230}	0.3502	0.3574	0.6390

With the parameter error, a measurement error of one sigma for V_{m735} becomes 2.6310 *sigma. Thus, an error of 7.35kV (or 1%) becomes in this case 19.3kV (or 2.6%).

From the above example, it is clear that tuning of the weights to reduce sensitivity to hidden topology errors in the Q-V model and to constrain the errors to particular regions of the system is not an easy task. The next section proposes a modification of the WLS algorithm that seeks the Dispatcher solution in presence parameter error should that solution exists.

VI. A New DWLS State Estimation Algorithm

When some of the assumptions on which are based the state estimator are violated due for example to parameter or topological errors, gross errors on transformer taps and positive sequence transformer model inaccuracies, the performance of the Q-V component of the state estimator can significantly deteriorate. In these cases, the normal equations given by (3) may possess several roots and the Gauss-Newton iterative algorithms may converge to one strongly biased solution that is not detected as such by the residual tests. It is found that this problem may not be overcome by adding new measurements or modifying the measurement configuration. To seek a solution foreseen by the dispatcher based on his belief that some voltage measurements are good and accurate, we propose to solve the Q-V component of the decoupled normal equation via the following DWLS iterative algorithm:

$$\Delta V^{(k)} = (D_V + H_{QV}^T R_{QV}^{-1} H_{QV})^{-1} H_{QV}^T R_{QV}^{-1} \Delta z_{QV}^{(k)}, \qquad (9)$$

where D_V is a matrix of weights associated with all the bus voltages increments. The idea is to drive the solution of important variables (voltages or flows) to a desirable solution, should that solution exists among the multiple roots of the normal equation (3) induced by the parameter or topology errors. However, when there are no parameter gross errors, the DWLS iterative algorithm converges to the same solution as the original Gauss-Newton method, even in presence of bad measurements. Consequently, the conventional bad data detection and identification procedure based on the weighted or the normalized residuals is not affected. Another interesting property of the DWLS algorithm is that it improves on the condition number of the gain matrix since the D_V positive weights are added to its diagonal elements; the positive definiteness of the matrix to be inversed in (9) is reinforced.

Let us now demonstrate the performance of the DWLS algorithm on the Hydro-Quebec subsystem displayed in Fig. 1 with a 50-MVar shunt parameter error on bus m230 as described in Section IV. For this case, the dispatcher's desire is to force the voltage state estimates on the 735-kV subsystem to be close to the voltage metered values while relaxing the voltage solution on the 230 kV subsystem. To do just that, the diagonal entries of D_V associated with the 735-kV voltages are made 100 times larger than those of the 230-kV voltages. Specifically, the former are set equal to the norm of Q-V gain matrix, $H_{QV}^T R_{QV}^{-1} H_{QV}$, while the latter weights are scaled down by a factor of 100 from that norm. The norm of a matrix is here defined as the largest sum of its column entries.

Table IV displays the error attenuation of the DWLS algorithm in presence of the shunt parameter error. We observe that the voltage error on V_{m735} is limited to 1.1343 x 7.35 kV = 8.3kV instead of 19.3kV. Of course, the errors are more important on the reactive power flows because the forced to get closer to the 735-kV voltage measurements. While the voltage solution is now acceptable for the dispatcher, it is nearly impossible to identify the value of the shunt reactance that needs to be corrected because all the solutions provided by the DWLS algorithm for different positions of the 3 circuit breakers of the reactor shunts are detected as valid by the residual tests. This possible failure must be taken into consideration when using a generalized state estimator such as the one promoted in [8].

VII. Conclusions

The paper has showed that in presence of small shunt parameter errors, the normal equation may exhibit multiple roots and the Gauss-Newton iterative algorithm may converge to a strongly biased Q-V solution that is not detected as such by the residual statistical tests. Our study has revealed that the manipulation of the measurement error variances is a necessary but not a sufficient condition to cope with modelling errors. Similar problems occur whether the solution is coupled or not, and whether the gain matrix is updated at each iteration or held constant.

To overcome this difficulty, a DWLS algorithm is proposed. This algorithm allows the dispatcher to choose appropriate weights for the state voltages that force the algorithm to converge to a desired solution, should that solution exists. The proposed DWLS algorithm has the advantage of offering a simple implementation for the current WLS algorithm. This calls for further research and development.

Table IV
DWLS error attenuation.

z	Without topology error	With topology error
Q_{km735}	0.2533	2.7949
V_{k735}	0.6320	0.8952
$\boldsymbol{V_{m735}}$	0.6632	**1.1343**
Q_{km230}	0.6562	0.9779
Q_{mk230}	0.6769	1.1129
Q_{k230}	0.4235	0.6168
V_{k230}	0.6269	1.6873
V_{m230}	0.6134	1.7606

References

[1] E. Handschin and E. Kliokys, "Transformer Tap Position Estimation and Bad Data Detection using Dynamic Signal Modeling," *IEEE Trans. on Power Systems*, Vol.10, No. 2, pp. 810-817, May 1995.

[2] P. A. Teixeira et al., "State Estimation of Voltage and Phase-Shift Transformer Tap Settings," *IEEE Trans. on Power Systems*, Vol.7, No.3, pp.1386-1393, Aug. 1992.

[3] P. Zarco and A. G. Exposito, "Power System Paramter Estimation: A Survey," *IEEE Trans. on Power Systems*, Vol. 15, No. 1, pp.216-222, Feb. 2000.

[4] I. W. Slutsker and K.A. Clements, "Real-time Recursive Parameter Estimation in Energy Management Systems," *IEEE Trans. on Power Systems*, Vol. 11, No. 3, pp. 1393-1399, Aug. 1996.

[5] W.-H E. Liu, F.F. Wu, S.-M. Lun, "Estimation of Parameter Errors from Measurement Residuals in State Estimation," *IEEE Trans. on Power Systems*, Vol 7, No 1, pp. 81-89, 1992.

[6] L. Mili, G. Steeno, F. Dobraca, D. French, “A Robust Estimation Method for Topology Error Identification,” *IEEE Trans. on Power Systems*, Vol 14, No 4, pp. 1469-1476, Nov. 1999.

[7] C. W. Hansen, A.S. Debs, “Power System State Estimation using Three-Phase Models,” *IEEE Trans. on Power Systems*, Vol 10, No 2, pp. 818-824, 1995.

[8] O. Alsaç N. Vempati, B. Stott, A. Monticelli, “Generalized state estimation,” *IEEE Tran.s on Power Systems*, Vol. 13, No. 3, pp. 1069–1075, 1998.